

**Proceedings of The Canadian Society for Mechanical Engineering International Congress 2018**  
**CSME International Congress 2018**  
**May 27-30, 2018, Toronto, On, Canada**

## MODELING VISCOELASTOMERS WITH NONLINEAR VISCOSITY

Jianyou Zhou, Liying Jiang and Roger E. Khayat  
 Department of Mechanical and Materials Engineering  
 The University of Western Ontario  
 London, Ontario N6A 6B9, Canada  
 lyjiang@eng.uwo.ca

**Abstract**— Consisting of highly mobile and flexible polymer chains, elastomers are known to exhibit viscoelastic behavior. Adopting concepts from the theory of polymer dynamics and finite-deformation viscoelasticity, this work presents a micro-macro constitutive model to investigate the viscoelastic behavior of elastomers, in which the material viscosity varies with the macroscopic deformation. The developed model is then applied to study the stress response of elastomers. From the simulation results, it is observed that the developed model exhibits strong capability of capturing the typical response behaviors of elastomers (e.g., strain-softening behavior). A comparison of the stress responses between linear and nonlinear viscosity is also considered in this work. The modeling framework in this paper is expected to provide a general approach and a platform to analyze the viscoelastic behavior of rubber-like materials with nonlinear viscosity.

*Elastomers; viscoelasticity; finite-deformation; nonlinear viscosity;*

### I. INTRODUCTION

Elastomers, capable of sustaining exceptionally large deformation, have extensive applications in engineering and industrial fields, such as flexible joints, automotive products, soft robots, artificial muscles and vibration isolators [1]. Formed by the cross-linking of highly mobile and flexible polymer chains, elastomers are hyperelastic and highly viscoelastic. These two major characteristics strongly affect the response of elastomers and have attracted much interest from the research community.

In the literature, numbers of constitutive models have been developed to capture the hyperelastic behavior of elastomers. These available models are established mainly based on two approaches: continuum mechanics treatments and statistical mechanics treatments. Developed through continuum mechanics framework, the phenomenological models assume that the hyperelastic properties of the material can be described by a strain energy function [2-3]. On the other hand, the hyperelastic constitutive models based on statistical treatments link the macroscopic response of the materials to their microstructure [4-5].

As for modeling the viscosity of elastomers, extensive research is also available in the literature. For example, phenomenological models that adopt thermodynamics evolution laws have been developed to tackle the inelastic deformation and viscous effect of elastomers, where the time-dependent strain variables are determined by the evolution laws [6-7]. Nevertheless, in these phenomenological models, details of the microstructure of the material related to the viscosity are not involved. Therefore, to reveal the physical mechanisms of the viscosity of the material, concepts from polymer dynamics [8] have been adopted later to develop the micromechanism inspired viscoelasticity models [9-10]. Although both the phenomenological models and the micromechanism inspired viscoelasticity models work well for fitting certain experimental data, they cannot capture the nonlinear viscosity of the material (viscosity varies with the deformation).

This motivates us to revisit the theory of polymer dynamics and the state-of-the-art theoretical framework of finite-deformation viscoelasticity to develop a micro-macro constitutive model, which aims to capture the viscoelastic deformation of elastomers with consideration of their nonlinear viscosity.

### II. THEORETICAL FRAMEWORK

#### A. Continuum Mechanics Framework

Following the pioneering works of Sidoroff [11], and Reese and Govindjee [7], it is assumed that the elastomer comprises an elastic polymer ground network and a viscous polymer subnetwork, which can be represented by the rheological model shown in Figure 1. Polymer network A is a purely elastic network, while network B is a viscous network. Consider a material point P in the reference configuration denoted by its position vector  $\mathbf{X}$ . When the elastomer is subject to external loads, point P moves to position  $\mathbf{x}$  in the current configuration. Then the total deformation gradient tensor  $\mathbf{F}$  is defined as  $\mathbf{F} = \nabla_{\mathbf{x}}(\mathbf{X}, t)$ . Since the deformation is applied to both polymer networks,  $\mathbf{F}_A = \mathbf{F}_B = \mathbf{F}$ . Borrowing a concept from finite-deformation plasticity, the deformation gradient tensor of network B can be further multiplicatively split into two parts, i.e.,  $\mathbf{F}_B = \mathbf{F}_B^e \mathbf{F}_B^i$ . Here,  $\mathbf{F}_B^e$  represents the deformation gradient of

the spring and  $\mathbf{F}_B^i$  denotes the deformation gradient of the dashpot. Adopting the rheological model in Fig. 1, the total Helmholtz free energy density of the elastomer is expressed as

$$W(\mathbf{F}_A, \mathbf{F}_B^e) = W_A(\mathbf{F}_A) + W_B(\mathbf{F}_B^e), \quad (1)$$

where  $W_A$  and  $W_B$  are the strain energy densities of the springs of network A and B, respectively [12-13]. Then the Cauchy stress tensor  $\boldsymbol{\sigma}$  and the first Piola-Kirchhoff stress tensor  $\mathbf{P}$  are given as

$$\mathbf{T} = J^{-1} \frac{\partial W_A(\mathbf{F}_A)}{\partial \mathbf{F}} \mathbf{F}^T + J^{-1} \frac{\partial W_B(\mathbf{F}_B^e)}{\partial \mathbf{F}} \mathbf{F}^T \quad (2)$$

and

$$\mathbf{P} = J\mathbf{T}\mathbf{F}^{-T}. \quad (3)$$

Moreover, the internal variables  $\mathbf{F}_B^e$  and  $\mathbf{F}_B^i$  must satisfy the following thermodynamic evolution equation, i.e.,

$$-\frac{1}{2}\mathbf{F}_B \frac{d[(\mathbf{C}_B^i)^{-1}]}{dt} (\mathbf{F}_B)^T (\mathbf{b}_B^e)^{-1} = \gamma^{-1} : \boldsymbol{\tau}_B. \quad (4)$$

Here,  $\boldsymbol{\tau}_B = 2\mathbf{F}_B^e \frac{\partial W}{\partial \mathbf{C}_B^e} (\mathbf{F}_B^e)^T$ ,  $\mathbf{b}_B^e = \mathbf{F}_B^e (\mathbf{F}_B^e)^T$ ,  $\mathbf{C}_B^i = (\mathbf{F}_B^i)^T \mathbf{F}_B^i$

and  $\gamma^{-1}$  takes the form

$$\gamma^{-1} = \frac{1}{2\eta_B} \left( \mathbf{I}^4 - \frac{1}{3} \mathbf{I} \otimes \mathbf{I} \right), \quad (5)$$

where  $\eta_B$  is the viscosity of the viscous polymer subnetwork B,  $\mathbf{I}^4$  is the fourth order symmetric identity tensor and  $\mathbf{I}$  is the second order identity tensor [7].

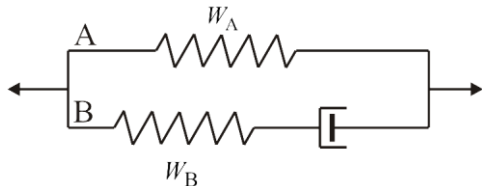


Figure 1. The rheological model of viscoelastic elastomers under finite-deformation.

### B. Nonlinear Viscosity

To obtain the stress with (2), (3), (4) and (5), the viscosity  $\eta_B$  of the viscous network must be constitutively prescribed first. Following Doi and Edwards [8],  $\eta_B$  can be expressed in terms of the shear relaxation modulus  $G_r$ , i.e.,

$$\eta_B = \int_0^\infty G_r dt. \quad (6)$$

In the short time-scale ( $t < \tau^e$ ),  $G_r$  is related to the microstructural parameters of the polymer network as

$$G_r \cong n_B k_B T \left( \frac{\tau^e}{\tau^R} \right)^{1/2}, \quad (7)$$

where  $n_B$  is the number of chains per unit volume in subnetwork B,  $k_B$  is the Boltzmann constant,  $T$  is the temperature,  $\tau^R$  is the relaxation time of the contour length of the primitive chain, and  $\tau^e$  is the critical time that the Brownian motion is restricted by the topological constraints (tube-like region) of the polymer network.

However, in the long time-scale ( $t > \tau^e$ ), the polymer chains may reptate out of the topological constraints (the tube). When reptation occurs, the shear relaxation modulus  $G_r$  is proportional to the fraction  $\varphi(t)$  of the chain still in the tube, i.e.,

$$G_r \cong n_B k_B T \left( \frac{\tau^e}{\tau^R} \right)^{1/2} \varphi(t). \quad (8)$$

By solving the one-dimensional diffusion equation to obtain  $\varphi(t)$  and integrating the shear relaxation modulus in (6),

$$\eta_B = \frac{\zeta n_B^4 b_0^4}{12 \langle a \rangle^2} \left( \frac{\tau^e}{\tau^R} \right)^{1/2}, \quad (9)$$

where  $a$  is the tube diameter in the current configuration,  $\zeta$  is the monomer friction constant,  $b_0$  is the effective bond length between monomers, and  $\langle * \rangle$  is the expectation operation of parameter  $*$  [13].

Considering nonlinear viscosity,  $\langle a \rangle$  should vary with the deformation. Moreover, the mean diameter  $\langle a \rangle$  is linked to the square end-to-end distance of the primitive chain  $\mathbf{R}_{ee}^2$  and the primitive chain length  $L$  by  $\langle a \rangle = \langle \mathbf{R}_{ee}^2 \rangle / \langle L \rangle$ . Following Li et al. [14],  $\langle \mathbf{R}_{ee}^2 \rangle$  is obtained as

$$\langle \mathbf{R}_{ee}^2 \rangle = \int |\mathbf{F} \cdot \mathbf{R}|^2 f_0(\mathbf{R}) d^3 \mathbf{R}, \quad (10)$$

where  $f_0(\mathbf{R})$  is the statistical distribution function of the end-to-end vector. Also, the mean primitive chain length  $\langle L \rangle$  is given as

$$\langle L \rangle = \int \frac{|\mathbf{F} \cdot \mathbf{u}_0|}{4\pi} L_0 d^2 \mathbf{u}_0, \quad (11)$$

where  $\mathbf{u}_0$  is the initial tangent vector of the primitive chain in the reference configuration. Then the ratio of the tube diameter between the current configuration and the reference configuration is expressed as

$$\frac{\langle a_n \rangle}{a_0} = \frac{\int |\mathbf{F} \cdot \mathbf{R}|^2 f_0(\mathbf{R}) d^3 \mathbf{R}}{\langle \mathbf{R}_{ee}^2 \rangle_0 \int \frac{|\mathbf{F} \cdot \mathbf{u}_0|}{4\pi} d^2 \mathbf{u}_0}. \quad (12)$$

Here,  $a_0$  is the tube diameter in the reference configuration. Therefore, the deformation-dependent viscosity is given as

$$\eta_B = \frac{\eta}{\alpha(\mathbf{F})^2}, \quad (13)$$

where  $\eta = \frac{\zeta n_B^4 \rho_0^4}{12 a_0^2} \left( \frac{\tau^R}{\tau^e} \right)^{1/2}$  is the viscosity of the elastomer in

the reference configuration and  $\alpha(\mathbf{F}) = \frac{\int |\mathbf{F} \cdot \mathbf{R}|^2 f_0(\mathbf{R}) d^3 \mathbf{R}}{\langle \mathbf{R}_{ec}^2 \rangle_0 \int \frac{|\mathbf{F} \cdot \mathbf{u}_0|}{4\pi} d^2 \mathbf{u}_0}$

indicates the deformation-dependency.

### III. NUMERICAL SIMULATIONS

To test the modeling capacity of the theoretical framework developed above, the material models (the strain energy densities  $W_A$  and  $W_B$  in (1)) need to be prescribed first. In this work, the Gent strain energy density function [3] is chosen as  $W_A$ , i.e.,

$$W_A = -\frac{G^{EQ} J_{lim}}{2} \ln \left( \frac{J_{lim} - \lambda_1^2 - \lambda_2^2 - \lambda_3^2}{J_{lim}} \right). \quad (14)$$

Here,  $G^{EQ}$  is the shear modulus of polymer network A and  $J_{lim}$  is the material extensibility parameter. Also,  $\lambda_1$ ,  $\lambda_2$  and  $\lambda_3$  are the stretch ratios in three directions. We assume that  $W_B$  takes the same form as  $W_A$ , which gives

$$W_B = -\frac{G^{NEQ} J_{lim}}{2} \ln \left[ \frac{J_{lim} - (\lambda_1^e)^2 - (\lambda_2^e)^2 - (\lambda_3^e)^2}{J_{lim}} \right], \quad (15)$$

where  $G^{NEQ}$  is the shear modulus of polymer network B.

Considering uniaxial tension,  $\lambda_1 = \lambda$ ,  $\lambda_2 = \lambda_3 = 1/\sqrt{\lambda}$ ,  $\lambda_1^e = \lambda^e$  and  $\lambda_2^e = \lambda_3^e = 1/\sqrt{\lambda^e}$ . From (2) and (3), the dimensionless nominal stress is obtained as

$$\frac{P_{11}}{G} = \frac{\chi J_{lim} (\lambda - \lambda^{-2})}{J_{lim} - 2\lambda^{-1} - \lambda^2 + 3} + \frac{(1-\chi) J_{lim} [\lambda (\lambda^i)^{-2} - \lambda^{-2} \lambda^i]}{J_{lim} - 2\lambda^{-1} \lambda^i - \lambda^2 (\lambda^i)^{-2} + 3}, \quad (16)$$

where  $G = G^{EQ} + G^{NEQ}$  and  $\chi = G^{EQ}/G$ . Also, the thermodynamic evolution equation gives that

$$\frac{d\lambda^i}{dt} = \frac{J_{lim} \lambda^i \alpha(\mathbf{F})^2}{3\tau [J_{lim} - 2\lambda^i \lambda^{-1} - \lambda^2 (\lambda^i)^{-2} + 3]} [\lambda^2 (\lambda^i)^{-2} - \lambda^i \lambda^{-1}]. \quad (17)$$

Here,  $\tau = \eta/G^{NEQ}$  is the relaxation time.

Fig. 2 depicts the dimensionless nominal stress  $P_{11}/G$  as a function of the stretch ratio of the elastomer at four different stretching rates, i.e.,  $|\dot{\lambda}| = 0.01/s$ ,  $|\dot{\lambda}| = 0.03/s$ ,  $|\dot{\lambda}| = 0.05/s$  and  $|\dot{\lambda}| = 1/s$ . It can be seen that the loading and unloading curves overlap at large stretch ratios when the stretching rates are relatively low (0.01/s ~ 0.05/s). According to (13), the viscosity  $\eta_B$  is inversely proportional to the second power of

$\alpha(\mathbf{F})$ . Therefore, the viscosity of the elastomer is exceptionally low at large stretch ratios, which leads to much faster relaxation of the polymer chains, thus causing the loading and unloading curves to overlap. However, when the stretching rate is high (e.g., 1/s), a wider gap between the loading and unloading curves appears since the elastomer has less time to relax during the loading path. To further examine the effect of the nonlinear viscosity on the stress response of the elastomer, Fig. 3 depicts the dimensionless nominal stress  $P_{11}/G$  obtained with  $\eta_B$  and  $\eta$ , respectively. A higher degree of strain-softening behavior is observed from the nonlinear viscosity case. Moreover, as the stretching rate increases, the stress difference between two cases becomes larger. Therefore, it is essential to consider the nonlinear behavior of the material viscosity in analyzing the stress response of elastomers, or it may lead to significant error in calculation. In Fig. 2 and Fig. 3, the material parameters are selected as  $\chi=0.5$ ,  $J_{lim}=110$  and  $\tau=500s$  [12-13].

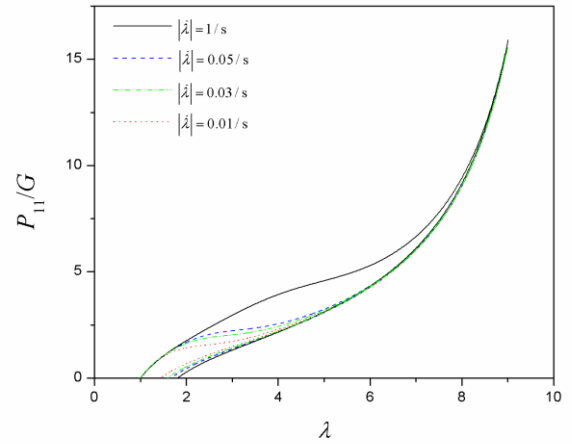
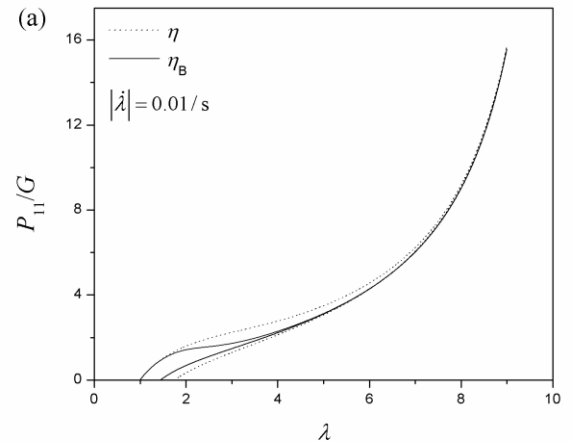


Figure 2. Stress response of the elastomer at different stretching rates.



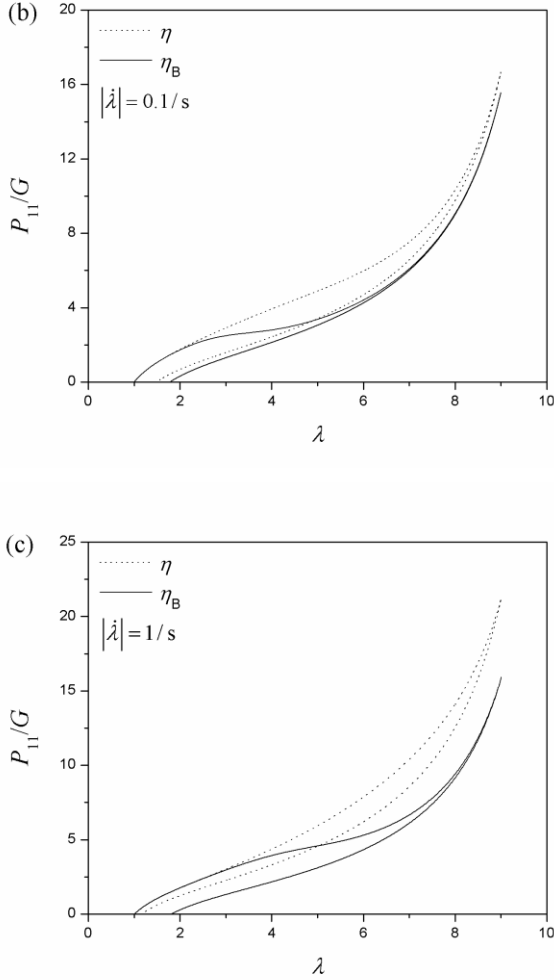


Figure 3. Comparison of the stress response between linear and nonlinear viscosity. (a)  $|\dot{\lambda}|=0.01/s$ , (b)  $|\dot{\lambda}|=0.1/s$  and (c)  $|\dot{\lambda}|=1/s$ .

#### IV. CONCLUSION

Based on the theory of polymer dynamics and finite-deformation viscoelasticity, a micro-macro constitutive model is developed to investigate the stress response and relaxation of elastomers under large deformation. For the developed model, all the material parameters have a microscopic foundation or physical meanings. Moreover, incorporating the nonlinear material viscosity into the continuum mechanics framework for finite-deformation viscoelasticity, the developed model can

adopt most of strain energy density functions for hyperelastic solids and thermodynamics evolution laws of viscoelastic materials. From our simulation results, it is found that the developed model can better capture the strain-softening behavior of elastomers, which could be explained by the nonlinear viscosity of the material. In summary, the developed modeling framework is anticipated to provide significant guidelines for studying the viscoelastic behavior of elastomers.

#### ACKNOWLEDGMENT

This work is supported by Natural Sciences and Engineering Research Council of Canada (NSERC).

#### REFERENCES

- [1] D. Rus, and M. T. Tolly, "Design, fabrication and control of soft robots," *Nature*, vol. 521, pp. 467-475, 2015.
- [2] M. C. Boyce, and E. M. Arruda, "Constitutive models of rubber elasticity: a review," *Rubber Chem. Technol.*, vol. 66, pp. 754-771, 2000.
- [3] A. N. Gent, "A new constitutive relation for rubber," *Rubber Chem. Technol.*, vol. 69, pp. 59-61, 1996.
- [4] E. M. Arruda, and M. C. Boyce, "A three-dimensional constitutive model for the large stretch behavior of rubber elastic materials," *J. Mech. Phys. Solids*, vol. 41, pp. 389-412, 1993.
- [5] J. D. Davidson, N. C. Goulbourne, "A nonaffine network model for elastomers undergoing finite deformations," *J. Mech. Phys. Solids*, vol. 61, pp. 1784-1797, 2013.
- [6] J. Lubliner, "A model of rubber viscoelasticity," *Mech. Res. Commun.*, vol. 12, pp. 93-99, 1985.
- [7] S. Reese, and S. Govindjee, "A theory of finite viscoelasticity and numerical aspects," *Int. J. Solids Struct.*, vol. 35, pp. 3455-3482, 1998.
- [8] M. Doi, and S. F. Edwards, *The theory of polymer dynamics*, Oxford: Clarendon, 1986.
- [9] C. Miehe, and S. Göktepe, "A micro-macro approach to rubber-like material. Part II: the micro-sphere model of finite rubber viscoelasticity," *J. Mech. Phys. Solids*, vol. 53, pp. 2231-2258, 2005.
- [10] C. Linder, M. Tkachuk, and C. Miehe, "A micromechanically motivated diffusion-based transient network model and its incorporation into finite rubber viscoelasticity," *J. Mech. Phys. Solids*, vol. 59, pp. 2134-2156, 2011.
- [11] F. Sidoroff, "Un modèle viscoélastique non linéaire avec configuration intermédiaire," *J. Méc.*, vol. 13, pp. 679-713, 1974.
- [12] W. Hong, "Modeling viscoelastic dielectrics," *J. Mech. Phys. Solids*, vol. 59, pp. 637-650, 2011.
- [13] J. Zhou, L. Jiang, and R. E. Khayat, "A micro-macro constitutive model for finite-deformation viscoelasticity of elastomers with nonlinear viscosity," *J. Mech. Phys. Solids*, vol. 110, pp. 137-154, 2018.
- [14] Y. Li, S. Tang, M. Kroger, and W. K. Liu, "Molecular simulation guided constitutive modeling on finite strain viscoelasticity of elastomers," *J. Mech. Phys. Solids*, vol. 88, pp. 204-226, 2016.